

Lateral Iontophoretic Solute Transport in Skin

Pamela M. Lai,¹ Yuri G. Anissimov,¹ and Michael S. Roberts^{1,2}

Received September 29, 1998; accepted October 23, 1998

Purpose. The lateral iontophoretic transport of three solutes (sodium, ethanolamine, lidocaine) from an active electrode through skin and other tissues to an indifferent electrodes was investigated.

Methods. Anodal epidermal iontophoresis was carried out on an *in vivo* rat model using constant direct current of 0.38 mA/cm². Cells were fixed on the epidermis of anesthetized rats at distances of adjacent, 3 cm and 7 cm apart. After iontophoresis, tissues were dissected at 1 cm intervals between the electrodes. Concentrations of the radiolabelled solutes in tissues were determined by liquid scintillation counting or gamma counting.

Results. The concentration of each solutes in the epidermis, dermis and other tissues was found to decrease in an exponential manner with lateral distance from the active electrode to the indifferent electrode. The detectable lateral distance for ethanolamine and lidocaine was less than 2 cm from the donor sites, at which distance the concentrations were not significantly different to those found in the corresponding contralateral site. The lateral drift velocities for all solutes in the epidermis and dermis were consistent with diffusivities of the order of 10⁻⁶ cm²/s. The drift velocity of sodium was greater than either lidocaine or ethanolamine.

Conclusions. The decline in solute concentration with lateral distance is mainly due to clearance from the site of application by the skin's microcirculation and decreases with distance from the active electrode until a baseline concentration, similar to the contralateral tissue concentration is reached.

KEY WORDS: iontophoresis; epidermis; dermis; clearance; lateral transport; velocity.

INTRODUCTION

Iontophoresis is the technique of transporting ionized solutes across membranes, such as epidermis, using an electrical potential, thus enhancing the delivery of ionized drugs across intact skin.

Epidermal transport of solutes by iontophoresis is dependent on many factors, including solute physicochemical factors (ionic charges, the presence of extraneous ions, pH of the donor solution, ionic strength, solute concentration, buffer constituents, chemical structure of the solute and conductivity); physiological factors (skin region—density of appendages, age, sex, race, hydration of the skin, delipidization—pretreatment of the skin with ethanol, fluidisation of lipids and permeability of skin) and electrical factors (current density, nature of electrodes, duration of treatment, nature of current (1–2).

Riviere *et al.* (3–4) has suggested that solutes delivered by iontophoresis accumulate in the dermis prior to absorption

by the blood supply. A number of studies from our group have examined tissue levels below an active electrode in terms of mechanism of transport, role of blood flow and solute structure (5–10). Singh & Roberts (5) have suggested that deeper tissue levels after iontophoresis mainly reflect passive diffusion or convective blood flow. Cross & Roberts (10) have shown that larger solutes have higher tissue concentrations than the smaller solutes.

Whilst the transport of solutes below an active electrode after epidermal iontophoresis is relatively well studied, limited information is available on the extent of transport in the tissues between the electrodes. A number of studies have shown that negligible concentrations of solute are found in the electrode solution or in tissues below the indifferent electrode after iontophoresis (5). In principle, some solute should be transported into tissues in the path of the iontophoretic current.

In this study, we examined the extent of transport of three solutes (sodium, ethanolamine and lidocaine) into tissues intermediate between active and indifferent electrodes following anodal iontophoresis in an *in vivo* rat model. A model was derived to interrelate the extent of this transport with clearance of the solute from the epidermis and dermis.

THEORETICAL SECTION

When a solution of solute of concentration C_o is applied to the epidermis and a potential difference is applied across an electrode in the solution and an indifferent electrode, the solute will be lost from the solution at a rate constant k_a to yield a concentration $C(t)$ at any time:

$$C_c(t) = C_o \exp(-k_a t) \quad (1)$$

where $k_a = Cl_c/V_c$ and Cl_c is clearance from cell of volume V_c due to iontophoresis. Cl_c can be defined in terms of the electric field in stratum corneum E_{sc} as:

$$Cl_c = \frac{DzE_{sc}F}{RT} A_c \quad (2)$$

where D is the diffusion coefficient, z is the valency of the solute, F is Faraday's number, R is the universal gas constant, T is the temperature and A_c is the area of the skin in contact with the cell.

Solute Transport Through Epidermis

Following the approach of Singh & Roberts (5), the skin is modelled as a set of well stirred compartments, with the concentration in the epidermis under the cell ($x = 0$) being:

$$V_e \frac{dC_e}{dt} = Cl_c C_c(t) - Cl_e C_e - Av_e C_e \quad (3)$$

where C_c and C_e are the concentrations of the solute in the donor cell and epidermis, respectively, Cl_c and Cl_e are the clearances from the donor cell and epidermis, respectively, V_e is the volume of epidermis under the donor cell, A is the lateral area of epidermis and v_e is the drift velocity of the solute in the epidermis (Fig. 1). Substituting $C_c(t)$ from equation 1 into equation 3 yields on integration:

¹ Department of Medicine, University of Queensland, Princess Alexandra Hospital, Brisbane, Queensland 4102, Australia.

² To whom correspondence should be addressed. (e-mail: m.roberts@mailbox.uq.edu.au)

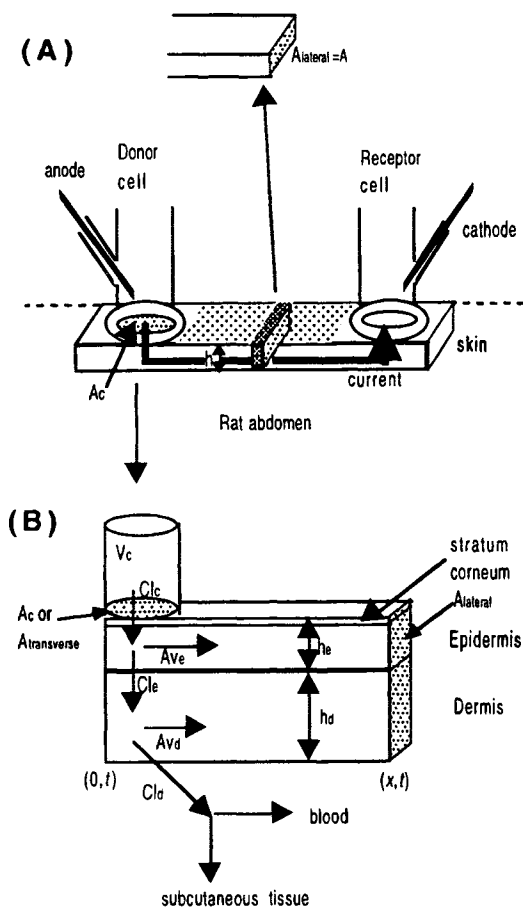


Fig. 1. Diagrammatic representation of iontophoresis and lateral transport in rat skin. (A) Electrode arrangement, and (B) Rate constants in process (see text for explanation). The current is assumed to be located mainly between the donor and receptor electrode.

$$C_e = \frac{V_c}{V_e} \frac{C_o k_a}{k_{el} - k_a} (e^{-k_a t} - e^{-k_{el} t}) \quad (4)$$

where $k_{el} = (Cl_e + Av_e)/V_e$.

When absorption is rate limited, $k_a \ll k_{el}$ and at moderate times (such that $t \gg 1/k_{el}$), equation 4 reduces to:

$$C_e = \frac{V_c}{V_e} \frac{C_o k_a}{k_{el}} e^{-k_{el} t} \quad (5)$$

and recognizing $k_{el} V_e = Av_e + Cl_e$, equation 5 can be expressed as:

$$(Av_e + Cl_e) = \frac{Cl_e C_c(t = 2h)}{C_e(t = 2h)} \quad (6)$$

Assuming $Cl_e \gg Av_e$ consistent with $A = A_{e,lateral} \gg A_{e,transverse} = A_c$, equation 6 can be written as:

$$Cl_e = \frac{Cl_e C_c(t = 2h)}{C_e(t = 2h)} \quad (7)$$

We now consider $C(x, t)$ in both the epidermis and dermis between two electrodes during iontophoresis. The transport of solute through the epidermis due to electric field may be defined

in terms of drift velocity v using a convection-reaction equation:

$$\frac{\partial C_e}{\partial t} = -\frac{\partial C_e}{\partial x} v_e - k_e C_e \quad (8)$$

where $\partial C_e / \partial t$ is the change in concentration of the solute with time, $\partial C_e / \partial x$ is the convective flow at distance x from the donor cell, k_e is the elimination rate constant of the solute from the epidermis and is expressed as $k_e = Cl_e / V_e$ and C_e is concentration of solute in the epidermis. Integrating equation 8 yields:

$$C_e(x, t) = e^{k_e / v_e x} \cdot C_e \left(0, t - \frac{x}{v_e} \right) \quad (9)$$

where $t > x / v_e$. Assuming $t \gg x / v_e$, equation 9 can be simplified to:

$$C_e(x, t) = C_e(0, t) e^{-k_e / v_e x} \quad (10)$$

Solute Transport Through Dermis

The transport of solute through the dermis is given by:

$$\frac{\partial C_d}{\partial t} = -\frac{\partial C_d}{\partial x} v_d - k_d C_d + \frac{h_e}{h_d} k_e C_e \quad (11)$$

where $\partial C_d / \partial t$ is the change in concentration of the solute with time in the dermis, $\partial C_d / \partial x$ is the convective flow at distance x from the donor cell, k_d is the elimination rate constant of the solute from the dermis (= clearance from dermis Cl_d for a given volume of dermis V_d), v_d is the drift velocity of the solute in the dermis, C_d is concentration of solute in the dermis and h_e and h_d are the thickness of the epidermis and dermis, respectively.

Assuming that $h_e \ll h_d$, then the concentration of solute in the dermis can be expressed in a similar form as equation 8 and therefore assuming $t \gg x / v_d$, equation 11 can be expressed similarly to equation 10:

$$C_d(x, t) = C_d(0, t) e^{-k_d / v_d x} \quad (12)$$

In practice, the observed concentrations will consist of iontophoretically delivered solute plus solute delivered by the systemic circulation. Hence equations 10 and 12 are more correctly expressed as:

$$C_i(x, t) = C_i(0, t) e^{(k_i / v_i) x} + C_{\text{system}, i} \quad (13)$$

where C_{system} is the tissue concentration due to the systemic circulation of the solute and i is the epidermis or dermis.

A theoretical estimate of v_i is also possible from a knowledge of diffusion coefficient D , using:

$$v_i = \frac{EFD}{RT} = \frac{\rho_i IFD}{ART} \quad (14)$$

noting $E = \rho_i I / A$, where E is the electric field and ρ is the resistivity of the epidermis or dermis.

MATERIALS AND METHODS

Chemicals and Instruments

[^{14}C]Lidocaine HCl (specific activity 48 mCi/mmol, purity > 97%) and [^3H]ethanolamine (35 mCi/mmol) and $^{22}\text{NaCl}$ (2.3–46 Ci/mmol) were purchased from New England Nuclear

or Amersham. Tissue solubiliser, NCSII, and liquid scintillation cocktails (OCS and Emulsifier-Safe) were purchased from Amersham. HEPES (N-2-hydroxyethylpiperazine-N-2-ethan-sulphonic acid) buffer salt was purchased from Sigma Chemical Co. and all other chemical reagents were of analytical grade. Water was distilled and de-ionized using a Waters Milli-Q unit. The depilatory cream used was Nair (Carter-Wallace (Australia) Pty. Ltd). A liquid scintillation counter (Tri-carb 4000 series, United Technologies, Packard, USA) was used to determine the radioactivity of [¹⁴C]lidocaine and [³H]ethanolamine in the samples and a gamma counter (Cobra II, Packard Instruments, Australia) used for ²²Na samples. The constant current used in the experiments was generated by a custom-made constant-current source (Physical Sciences, Princess Alexandra Hospital).

Animals

Male Wistar rats (300–350 g) were used in the studies. The animals were housed under standard laboratory conditions (20.0 ± 0.5°C, relative humidity 55–75%) and supplied with a normal pellet diet and water ad libitum. All experiments had previously been approved by the Animal Experimentation Committee of the University of Queensland.

Methods

The rats were anaesthetised with azaperone (80 mg/kg i.p.) and ketamine HCl (130.5 mg/kg i.p.) and their body temperature maintained throughout the experiment at 37°C by placing them on a heating pad. Resistance between the cells were measured by measuring voltage with a multimeter. The hair on the dorsal area was clipped with electrical clippers, and any residual hair was removed by application of a depilatory cream (5). The depilated area was swabbed thoroughly with distilled deionized water to remove any traces of the depilatory. A donor glass absorption cell (internal diameter, 1.8 cm) was fixed to the epidermis of the abdomen using adhesive and warmed to 37°C by means of an external heating device (11). A receptor glass absorption cell was placed at distance of 0 (adjacent), 3 and 7 cm from the donor cell. A solution comprising of 2 ml 50 mM HEPES buffer, pH 6.3, spiked with [¹⁴C]lidocaine (5 µCi) and [³H]ethanolamine (10 µCi) or ²²NaCl (200 mCi), were placed in the donor cell and stirred by a glass stirrer driven by an external motor. A solution of 1 ml 20 mM isotonic HEPES, pH 7.4, was placed in the receptor cell. A silver (Ag) electrode (anode) was placed in the donor cell and the circuit completed by a AgCl electrode in the receptor cell. A current of 0.38 mA/cm² was applied between the two electrodes by a constant current generator.

Aqueous samples (10 µl) were removed from the donor cell at 0, 15, 30, 45, 60, 90, 120 min and placed in scintillation vials. The glass absorption cells were removed from the rat skin at the completion of the experiment (2 h), and the application area wiped dry with blotting paper. A blood sample was then taken from the tail vein and the animal sacrificed by cervical dislocation. Immediately thereafter, the tissues below the treated site, that is, skin, subcutaneous tissue, muscle lining or superficial muscle, muscle and fat pad, were removed by dissection and placed in preweighed scintillation vials (5). Similarly, tissues around the donor site, at intervals of 1 cm², are

removed at a distance from the donor to the receptor, as well as the tissues below the contralateral side. Dissection instruments were cleaned with alcohol soaked swabs between each tissue sample to prevent cross contamination of radiation. Epidermal and dermal layers were separated by exposure to concentrated ammonia fumes following the method of Kligman and Christophers (12). Tissues containing [¹⁴C]lidocaine or [³H]ethanolamine were solubilized with tissue solubilizer before counting in scintillation counter, and tissues containing ²²NaCl were counted directly in the gamma counter. Each study was performed in triplicate.

Potential Difference Between Cells

The voltage between the donor and electrode electrodes on the anaesthetized rat were measured using a multimeter, at various time intervals. After sacrificing the animal, the epidermis, dermis and subcutaneous fat were dissected and voltage between the two cells was measured. To examine the effect of the stratum corneum as the main barrier of the epidermis, the stratum corneum was removed by dermatoming, and again the voltage between the two cells was measured. The subcutaneous fat and tissues under the subcutaneous fat were then removed by dissection, and the potential difference measured. Resistance *R* was then calculated using Ohm's law, this measured potential difference (*U*) and the predefined constant current (*I*) i.e. $R = U/I$.

Sample Treatment

Aqueous samples (10 µl) removed from the donor glass cell were directly mixed with 5 ml of liquid scintillation cocktail, Emulsifier-Safe (Amersham Australia, Sydney) and counted in a liquid scintillation counter. The amount sampled from the donor cell was <5% of total cell volume. The tissue samples were solubilized with 1 ml of tissue solubiliser NCSII (Amersham Australia, Sydney) at 50°C for 6–8 h, longer where required, prior to the addition of 10 ml of organic scintillant OCS for beta scintillation counting.

Analysis

Zero-time samples from the cell were used to represent the initial solution concentration, and radioactivity in the tissues and plasma were converted to % of the initial solution concentration (concentration fraction).

According to equation 5, the drift velocity and hence the path of the solute during iontophoresis is dependent on the electric field and the diffusion coefficient. In this study, the electric field was calculated using:

$$E = \frac{U_{overall} - (U_{donor} + U_{receptor})}{d} \quad (15)$$

where $U_{overall}$ is the overall potential difference between the electrodes, U_{donor} is the drop in voltage in the donor cell, $U_{receptor}$ is the drop in voltage in the receptor cell and *d* is the distance between the electrodes.

Data Analysis

Nonlinear regressions were undertaken using Minim 3.0.9 (13). The data was weighted $1/y_{obs}$, consistent with the variance

of associated with radiolabeled solutes used in the majority of the data studied.

RESULTS AND DISCUSSION

The experimental conditions chosen for the present study included the direct application of current at 0.38 mA/cm^2 , well within the maximum current of 0.5 mA/cm^2 reported to be tolerant by humans before any discomfort is felt (14). The pH of the buffer used was pH 6.3, as at this pH, the solutes of interests are >97% ionized (pK_a lidocaine 7.9, pK_a ethanolamine 9.5).

Measurements of the potential difference in rat skin yielded an electric field E of 2 V/cm . A similar order of magnitude of electric field (1.2 V/cm) was calculated from literature data of human muscle (15).

Loss of Solute from the Donor

The % remaining of solutes from the donor site of [^3H]ethanolamine, [^{14}C]lidocaine and ^{22}Na with time during anodal iontophoresis is shown in Fig. 2. The % remaining-time profile of the three solutes were consistent with first order kinetics. The amount of ethanolamine, lidocaine and sodium lost from the donor cell after 2 h iontophoresis are 84.1%, 55.9% and 94.2% of initial concentration, respectively. There were no significant difference in loss of solutes from cell, at different distances at which the receptor electrode was placed from the donor electrode. The smallest solute sodium (MW 23) showed the highest flux, and lidocaine (MW 270) had the lowest flux. These results are consistent with our earlier studies (16–18) showing that iontophoretic transport decreases as the size of the solute increases. There were no significant loss observed from cells in the absence of iontophoresis (passive transport) after 2 h for ethanolamine, lidocaine and sodium.

Singh & Roberts (5) reported a loss of 25% of lidocaine during lidocaine iontophoresis. Cross & Roberts (10) observed loss from donor cell of ethanolamine and lidocaine to be 56.8% and 48.5%, respectively after 2 h iontophoresis, performed with donor solution at pH 7.4.

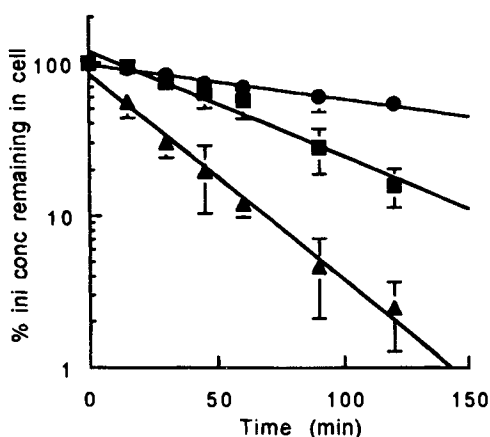


Fig. 2. Concentration (expressed as % of initial concentration) remaining in donor cell over time of (▲) sodium (mean \pm s.d., $n = 6$), (■) ethanolamine (mean \pm s.d., $n = 9$) and (●) lidocaine (mean \pm s.d., $n = 9$).

Concentration in the Underlying Tissues

Sodium

Figure 3A and B shows the fit of equation 13 to observed ^{22}Na concentrations at various lateral distances from the active electrode to the indifferent electrode in the epidermis and dermis, when the receptor electrode was placed adjacent to and at a distance of 7 cm from the donor electrode, respectively. The highest concentration of ^{22}Na was found in the epidermis under the donor (at the active electrode) site. Concentrations of Na then decrease exponentially with distance to become comparable to contralateral concentrations at about 2 cm from the donor site. Figure 3A and B show that the Na concentrations are similar in the contralateral dermal and epidermal tissue, consistent with no preferential binding in each tissues. The similarity in dermal and epidermal concentrations at distances more than 2 cm from the active electrode with concentrations in contralateral tissues suggests that these concentration mainly are from redistribution from the local blood supply. It is likely that the lateral concentration-distance profiles are tissue dependent in that the systemic Na concentrations accumulate gradually with time. Singh & Roberts (5–8) have shown that the observed extent of deep tissue penetration of salicylate and lidocaine is also time dependent. Deep tissue penetration is most evident at early times after dermal application. At longer times, recirculation from the systemic blood circulation dominates in determining the observed tissue concentrations.

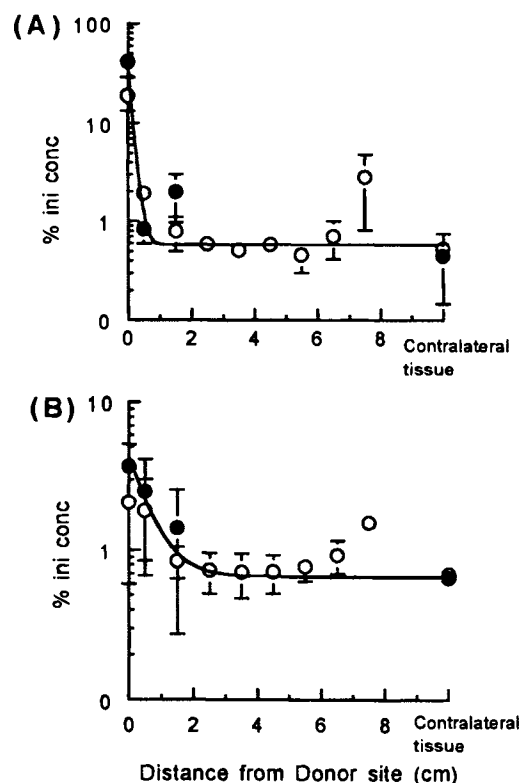


Fig. 3. Concentration (expressed as % of initial concentration) of ^{22}Na in tissue in treated and at intervals of 1 cm from the treated site to the receptor of (A) epidermis, and (B) dermis. (●) is the concentration when electrodes are adjacent to each other and (○) is the concentration when the electrodes are 7 cm apart (mean \pm s.d., $n = 3$), the solid line represents the regression estimated by equation 13.

Ethanolamine

Figure 4A, B and C shows the fit of equation 13 to [^3H]ethanolamine concentrations in the epidermis and dermis, when the receptor electrode was placed adjacent to and at a distances of 3 cm and 7 cm from the donor electrode, respectively. The epidermal and dermal concentration-distance profiles for ethanolamine are similar in shape to Na (Fig. 3) with concentrations in tissues greater than 2 cm from the active electrode being similar to that in contralateral tissue. The difference in epidermal and dermal concentrations is probably due to the differing affinity of ethanolamine for the tissues as (i) the contralateral tissues also differ by a similar order of magnitude and (ii) the epidermal and dermal concentrations of sodium (Fig. 3) and lidocaine (Fig. 5) do not show such differences. Figure 4D shows that all tissue concentrations can be superimposed irrespective of distance between electrodes. The superimposition is consistent with an identical constant current being used across each set of electrodes irrespective of the distance between the electrodes. Hence, the electric field-distance profile will be the same in the epidermis and dermis for each of these studies.

Lidocaine

Figure 5A, B and C shows fit of model to [^{14}C]lidocaine in the various tissues, when the receptor electrode was placed

adjacent to and at a distances of 3 cm and 7 cm from the donor electrode. Similar to the results of sodium and ethanolamine, the greatest concentration was found in the epidermis of the treated site, then decreasing until after a distance of 2 cm or greater from the donor site, when the concentrations are not significantly different from those found in contralateral tissue. The similar epidermal and dermal contralateral lidocaine concentrations suggest that there is not a selective binding of lidocaine for either the epidermis or dermis. Figure 5D shows the superimposed tissue concentrations at various distances between the electrodes.

Electrical Resistance of Tissues and Lateral Transport of Solutes

Our experiments on the electrical resistance across a transverse section of excised rat skin showed that the stratum corneum accounted for over half the electrical resistance in rat skin. When the stratum corneum was removed by dermatomy, the electrical resistance decreased. Hence, consistent with other studies, the stratum corneum is the main electrical resistance to solute transport into the skin (19–20). Whilst lateral epidermal and dermal concentrations arise from iontophoretic transport, it is less likely that iontophoresis account for the tissue concentration-distance profiles observed for the deeper tissues

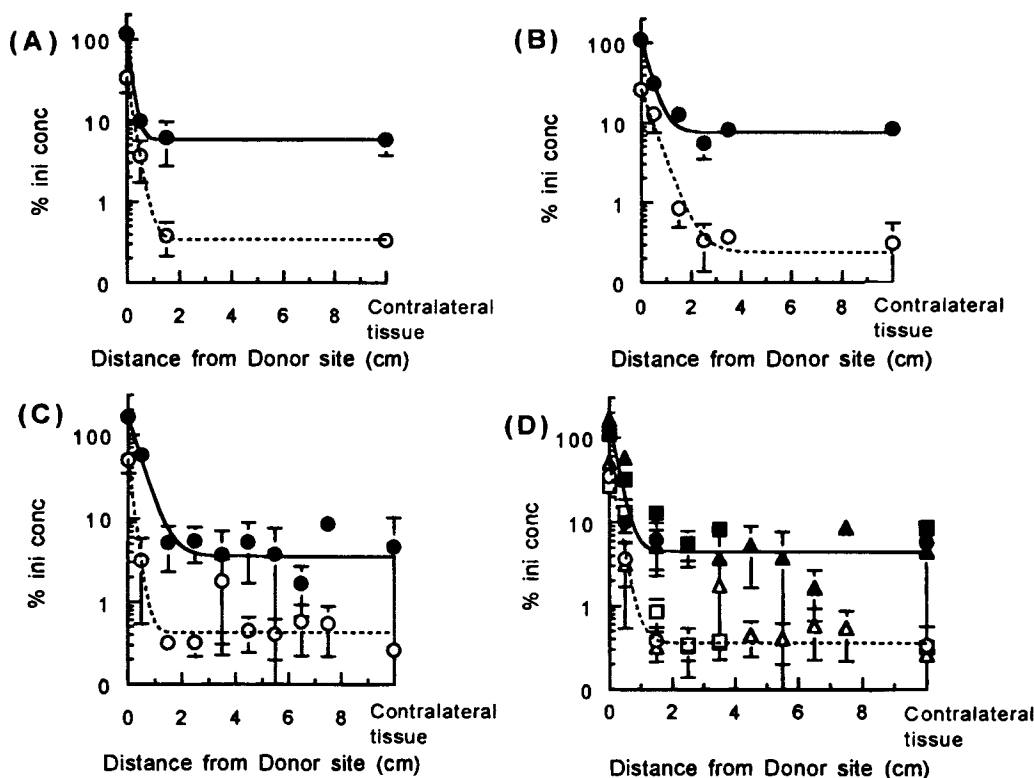


Fig. 4. Concentration (expressed as % of initial concentration) of [^3H]ethanolamine in tissue in treated and at intervals of 1 cm from the treated site to the receptor when electrodes are placed (A) adjacent to each other, (B) at a distance of 3 cm, (C) at a distance of 7 cm from each other, (●) is the concentration in the epidermis and (○) is the concentration in the dermis, the solid and dotted lines represent the regression estimated by equation 13 for epidermis and dermis, respectively, and (D) when all distances are superimposed (●) and (○) are the concentrations in the epidermis and dermis, cells placed adjacent to each other, respectively, (■) and (□) are the concentrations in the epidermis and dermis, cells placed 3 cm apart, respectively and (▲) and (△) are the concentrations in the epidermis and dermis, cells placed 7 cm apart, respectively (mean \pm s.d., $n = 3$).

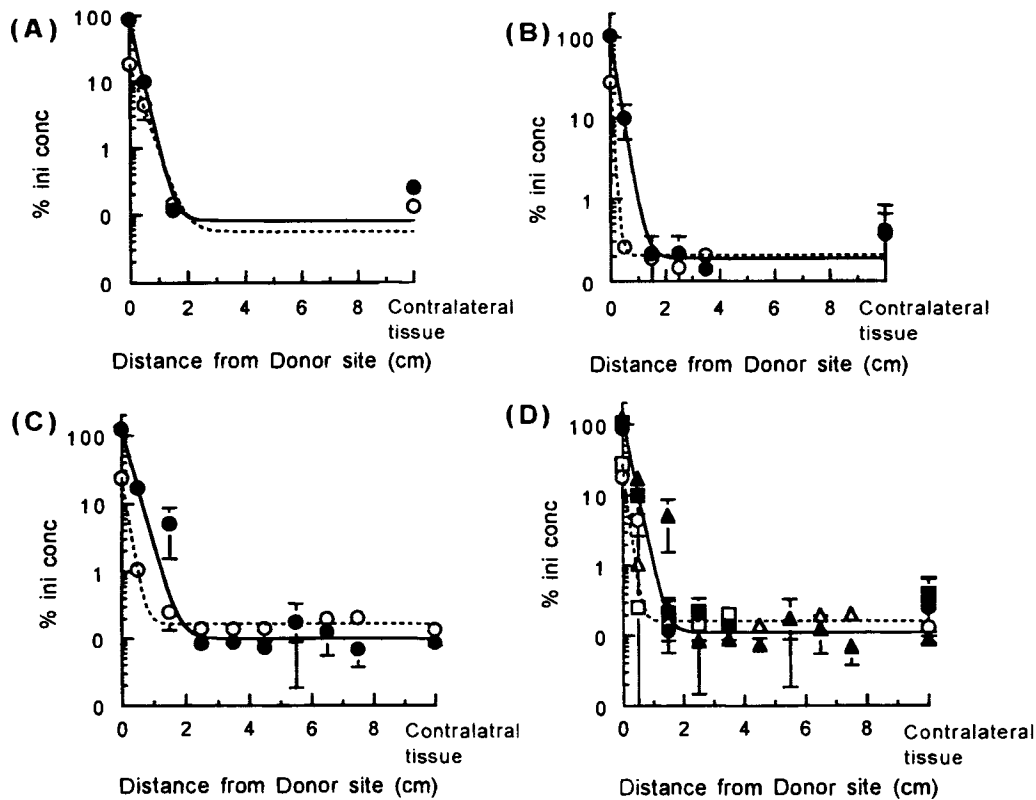


Fig. 5. Concentration (expressed as % of initial concentration) of $[^{14}\text{C}]$ lidocaine in tissue in treated and at intervals of 1 cm from the treated site to the receptor when electrodes are placed (A) adjacent to each other, (B) at a distance of 3 cm, (C) at a distance of 7 cm from each other, (●) is the concentration in the epidermis and (○) is the concentration in the dermis, the solid and dotted lines represent the regression estimated by equation 13 for epidermis and dermis, respectively, and (D) when all distances are superimposed (●) and (○) are the concentrations in the epidermis and dermis, cells placed adjacent to each other, respectively, (■) and (□) are the concentrations in the epidermis and dermis, cells placed 3 cm apart, respectively and (▲) and (△) are the concentrations in the epidermis and dermis, cells placed 7 cm apart, respectively (mean \pm s.d., $n = 3$).

(Fig. 6). Similar profiles (not shown) were found for electrode placements adjacent to and 3 cm apart. A more likely explanation is transport to the deeper tissues by diffusion and, possibly, convective blood flow as proposed for the transport of solutes into deeper tissues by Singh & Roberts (5,7–9) after passive dermal application. Singh & Roberts (5) found similar deep tissue concentrations after dermal and iontophoretic application to intact epidermis and suggested that all transport into deep tissues occurred by diffusion (or “convective” blood transport) and not by iontophoretic delivery. Our experiments suggest that subcutaneous fat has a lower electrical conductivity than other tissues. Consistent with this apparent lower conductivity, subcutaneous fat has been considered to be a “semi-” insulating layer, due to its low water content (15). Accordingly, we suggest that the stratum corneum offers the initial barrier for the entry of solutes into the skin by iontophoresis and that the epidermis and dermis are the main layers which conduct the iontophoretic current between the electrodes. Concentrations found in deeper tissues are probably due more to diffusion or “convective” blood transport from the upper layers than due to direct iontophoretic transport. At this stage, we do not have definitive evidence to define the relative contribution of iontophoresis and transverse diffusive or convective transport as determinants of the concentrations in the deeper tissues.

Solute Structure and Iontophoretic Transport

Whilst the iontophoretic transport of solutes across the stratum corneum is highly dependent on solute size (Fig. 1) (16–18), the clearances from sodium, ethanolamine and lidocaine from epidermis and dermis are relatively similar (Table I). Singh & Roberts reported clearances for lidocaine of 0.0065 ml/min from epidermis and 0.025 ml/min from dermis, respectively (5). These are similar to the values reported in Table I. They suggested that clearance in the deeper tissues are due to diffusion and removal by blood supply, with blood supply removal being the dominant process (5). Singh & Roberts (9) also reported that, due to the dominance of solute clearance by blood, the dependence of solute concentrations in anesthetized animal tissues were less evident those observed for sacrificed animals.

It has been suggested that the microcirculation in the absorption zone plays an important role in the uptake of solutes, particularly low molecular weight compounds (5,9,21), and the rate limiting step for high molecular weight solutes is tissue diffusion (22,23). Cross & Roberts (10) suggests that the presence of a viable blood supply significantly affects the distribution of applied solutes into underlying tissues during iontophoresis, with higher concentrations remaining in the

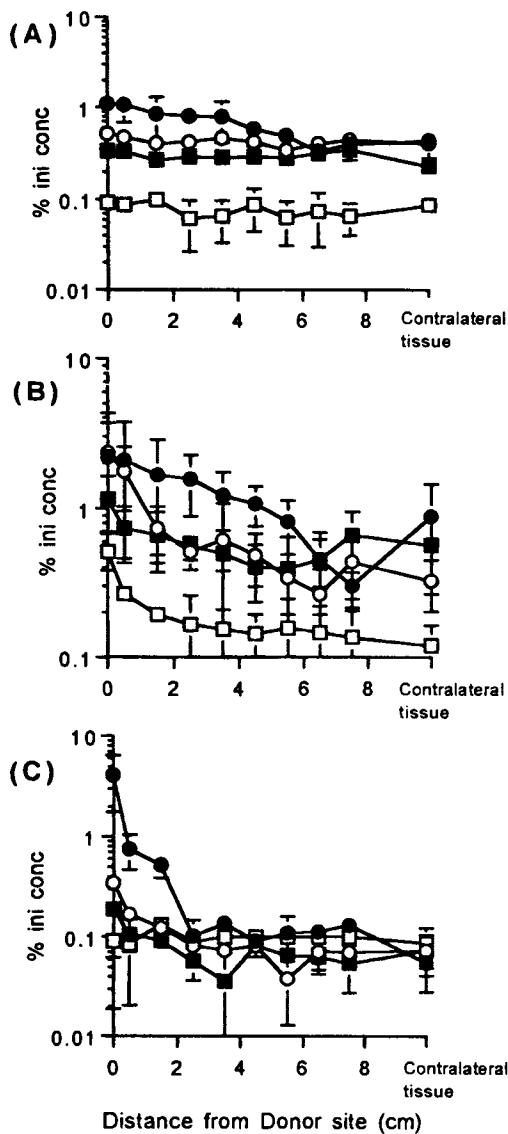


Fig. 6. Concentration (expressed as % of initial concentration) in deeper tissues when electrodes are placed 7 cm apart of (A) ^{22}Na , (B) ethanolamine, and (C) lidocaine. (●) is the concentration in subcutaneous fat, (○) is the concentration in superficial muscle, (■) is the concentration in muscle and (□) is concentration in fat pad. (mean \pm s.d., $n = 3$).

upper tissue layers where distribution in the blood is precluded. The smaller concentrations of sodium in other sites other than in the treated epidermis suggests that the blood flow played a significant effect in redistributing or eliminating the drug from the dermis. The lower dermal sodium concentrations relative to ethanolamine and lidocaine, may reflect the size dependence of clearance into the dermal blood supply. Singh & Roberts (9) have shown that solute clearance due to removal into the dermal blood supply increases as the size of the differing solute decreases.

Other Studies Measuring Lateral Transport

There was no significant concentrations (different from corresponding contralateral tissue) observed in either ethanolamine or lidocaine after a lateral distance of 2 cm from the donor cell, with concentrations in the epidermis and dermis decreasing with distance from the treated site at an exponential rate. Singh & Roberts (5) observed no salicylic acid or lidocaine in the tissues below the indifferent electrode after epidermal iontophoresis in rats. They also did not detect lidocaine in the indifferent electrode receptor solution. As well, Glikfeld *et al.* (24) also reported no morphine or clonidine in the tissues below the indifferent electrode after iontophoretic application to hairless mouse skin *in vitro*. Russo *et al.* (25) did not find evidence of lateral spread of anesthesia after iontophoretically applying lidocaine in human volunteers. These findings are consistent with the present work in that this work has shown that lateral spreading was limited to a small distance from the active electrode. None of the solutes were detected in the receptor solution of the indifferent electrode in this work. However, Glikfeld observed significant traces of morphine, clonidine and theophylline in their receptor *in vitro* (24,26). Singh and Roberts suggested that the differences are likely to be that in an *in vivo* model, the dermal blood supply offers a sink condition, compared with the close proximity of the donor and receptor solutions in the *in vitro* studies (5).

Lateral Drift Velocity

Table II shows the values for k/v based on the regressions for each solute the estimated values for drift velocity v using clearance values from Table I. Also included in this Table are the estimated diffusivities D based on equation 14. It is apparent that there was no significant difference between the drift velocity of the three solutes in the epidermis in terms of solute size

Table I. Epidermal and Dermal Clearances Calculated for Na, Ethanolamine, and Lidocaine from the Epidermis and Dermis

Solute	Distance between electrodes	$Cl_{\text{epidermis}}$ (ml/min) ^a (mean \pm s.d.)	Cl_{dermis} (ml/min) ^b (mean \pm s.d.)
Na ⁺	Adjacent	0.0045 \pm 0.0005	0.0511 \pm 0.0064
	7cm	0.0099 \pm 0.0003	0.0902 \pm 0.0047
Ethanolamine	Adjacent	0.0031 \pm 0.0004	0.0106 \pm 0.0089
	3cm	0.0033 \pm 0.0006	0.0138 \pm 0.0054
Lidocaine	7cm	0.0022 \pm 0.0009	0.0073 \pm 0.0023
	Adjacent	0.0071 \pm 0.0011	0.0340 \pm 0.0018
	3 cm	0.0059 \pm 0.0009	0.0224 \pm 0.0079
	7 cm	0.0049 \pm 0.0012	0.0257 \pm 0.0063

^a Calculated using equation 7.

^b Calculated using $Cl_d = (Cl_e C_e)/C_d$ ($t = 2\text{h}$).

Table II. Estimates of Solute Drift Velocity and Diffusivity Based on Nonlinear Regression of Epidermal and Dermal Concentration-Distance Profiles from Active Electrode

Solute		k/v^a (1/cm)	Drift velocity ^b (cm/min)	Diffusion coefficient (cm ² /s)	r ² for regression
Na ⁺	Epidermis	8.51 ± 4.44	0.044 ± 0.029	9.73 × 10 ⁻⁶	0.98
	Dermis	1.69 ± 0.62	0.202 ± 0.018	44.95 × 10 ⁻⁶	0.66
Ethanolamine	Epidermis	4.68 ± 0.83	0.033 ± 0.011	7.26 × 10 ⁻⁶	0.98
	Dermis	4.99 ± 0.86	0.013 ± 0.009	2.97 × 10 ⁻⁶	0.99
Lidocaine	Epidermis	4.79 ± 0.43	0.054 ± 0.007	11.96 × 10 ⁻⁶	0.99
	Dermis	8.30 ± 1.56	0.022 ± 0.016	4.92 × 10 ⁻⁶	0.99

^a From regression.

^b Calculated using equation 14, k/v and clearances from Table I.

(MW). However in the dermis, the velocity of sodium was significantly higher than either ethanolamine or lidocaine, as well as its own velocity in the epidermis. The high value for sodium in the dermis is probably an anomaly, the reason for which is ill defined. There was no significant difference between the velocity of ethanolamine and lidocaine in the epidermis and dermis. The diffusion coefficients estimated in Table II are in the order of 10⁻⁶ cm²/s.

In the iontophoresis of sodium, the epidermal and dermal concentration below the receptor cell were higher than those found in the contralateral tissue level (Fig. 3). We initially thought that this increase may have been a result of iontophoresis induced vasodilation (27). We therefore conducted a series of studies applying nitroglycerin ointment 0.2% as a topical vasodilator intermediate between the electrodes for the duration of the iontophoresis. However, no significant difference in tissues below the vasodilator and elsewhere was found. A more likely explanation for the selective increase of Na⁺ concentrations, as compared to lidocaine and ethanolamine, is the need to electrically neutralise the flow of Cl⁻ from the receptor into the tissues below as a result of the iontophoresis. The increase in sodium relative to other ions reflects its very high mobility (5.19 × 10⁻⁴ cm²V⁻¹s⁻¹ (28)), compared with lidocaine (2.0 × 10⁻⁴ cm²V⁻¹s⁻¹ (29)). It is suggested that Na⁺ migrates from the plasma to the receptor tissue site as a compensatory flux. The dominance of chloride transport across the receptor stratum corneum during iontophoresis would account for both the accumulation of Na⁺ in the receptor tissues and the negligible Na⁺ concentrations in the receptor solution. For less mobile ions, e.g. ethanolamine and lidocaine, this effect is not marked due to their low mobility and their much lower concentration in plasma (0.004 ± 0.0006 and 0.006 ± 0.001% initial concentration, for ethanolamine and lidocaine, respectively, n = 9, mean ± s.e.).

CONCLUSIONS

This study attempted to evaluate the lateral iontophoretic transport of three solutes, sodium, ethanolamine and lidocaine in tissue between an active and an indifferent electrode. According to the model derived for the pathway of solutes during iontophoresis, the concentration of solute decreased with distance from the active electrode in an exponential fashion due to clearance by the skin's microcirculation, until a baseline concentration, similar to the contralateral tissue concentration is reached. There was no significant difference in the drift

velocity of lidocaine and ethanolamine in either the epidermis or dermis.

ACKNOWLEDGMENTS

The authors wish to acknowledge the financial support of the National Health and Medical Research Council of Australia, the Princess Alexandra Hospital Foundation and the Queensland and Northern New South Wales Medical Research Foundation.

REFERENCES

1. M. S. Roberts, P. M. Lai, S. E. Cross, and N. H. Yoshida. Solute structure as a determinant of iontophoretic transport. In R. O. Potts and R. H. Guy (eds), *Mechanisms of Transdermal Drug Delivery*, Marcel Dekker, New York 1997 pp. 351-349.
2. P. M. Lai and M. S. Roberts. Iontophoresis. In M. S. Roberts and K. Walters (eds), *Dermatological Formulations and Toxicology*, Marcel Dekker, New York, 1998, pp. 379-422.
3. J. E. Riviere, B. Sage, and P. L. Williams. Effects of vasoactive drugs on transdermal lidocaine iontophoresis. *J. Pharm. Sci.* **80**:615-620 (1991).
4. J. E. Riviere, N. Monterio-Riviere, and A. Inman. Determination of lidocaine concentrations in skin after transdermal iontophoresis: Effects of vasoactive drugs. *Pharm. Res.* **9**:211-214 (1992).
5. P. Singh and M. S. Roberts. Iontophoretic transdermal delivery of salicylic acid and lidocaine to local subcutaneous structures. *J. Pharm. Sci.* **82**:127-131 (1993).
6. P. Singh and M. S. Roberts. Blood flow measurements in skin and underlying tissues by microsphere method: application to dermal pharmacokinetics of polar non-electrolytes. *J. Pharm. Sci.* **82**:873-873 (1993).
7. P. Singh and M. S. Roberts. Skin permeability and local tissue concentrations of non-steroidal anti-inflammatory drugs (NSAIDs) after topical application. *J. Pharmacol. Exp. Ther.* **268**:141-151 (1994).
8. P. Singh and M. S. Roberts. Dermal and underlying tissue pharmacokinetics of lidocaine after topical application. *J. Pharm. Sci.* **83**:773-782 (1994).
9. P. Singh and M. S. Roberts. Local deep tissue penetration of compounds after dermal application: structure-tissue penetration relationships. *J. Pharmacol. Exp. Ther.* **279**:908-917 (1996).
10. S. E. Cross and M. S. Roberts. The importance of dermal blood supply and the epidermis on the transdermal iontophoretic delivery of five monovalent cations. *J. Pharm. Sci.* **84**:1020-1027 (1995).
11. O. Siddiqui, M. S. Roberts, and A. Polack. The effect of iontophoresis and vehicle pH on the invitro permeation of lignocaine through human stratum corneum. *J. Pharm. Pharmacol.* **37**:732-734 (1985).

12. A. M. Kligman and E. Christophers. Preparation of isolated sheets of human stratum corneum. *Arch. Dermatol.* **88**:702–705 (1963).
13. R. D. Purves. Accuracy of numerical inversion of Laplace transforms for pharmacokinetic parameter estimation. *J. Pharm. Sci.* **84**:71–74 (1995).
14. H. A. Abramson and H. H. Gorin. Skin reactions IX. The electrophoretic demonstration of the patent pores of the living human skin; its relation to the charge of the skin. *J. Phys. Chem.* **44**:1094–1099 (1940).
15. L. A. Geddes and L. E. Baker. The specific resistance of biological material—a compendium of data for the biomedical engineer and physiologist. *Med. & Biol. Eng.* **5**:271–293 (1967).
16. M. S. Roberts, J. Singh, N. Yoshida, and K. I. Currie. Iontophoretic transport of selected solutes through human epidermis. In R. C. Scott, J. Hadgraft, and R. Guy (eds.), *Prediction of Percutaneous Absorption*; IBC Technical Services Ltd, London, 1990, pp. 231–241.
17. N. H. Yoshida and M. S. Roberts. Structure-transport relations in transdermal iontophoresis. *Adv. Drug Del. Rev.* **9**:239–264 (1992).
18. N. H. Yoshida and M. S. Roberts. Solute molecular size and transdermal iontophoresis across excised human skin. *J. Contr. Rel.* **25**:177–195 (1993).
19. M. S. Roberts. Targeted drug delivery to the skin and deeper tissues: role of physiology, solute structure and disease. *Clin. Exp. Pharmacol. Physiol.* **24**:874–879 (1997).
20. N. G. Turner and L. B. Nonato. Visualization of stratum corneum and transdermal permeation pathway. In R. O. Potts and R. H. Guy (eds), *Mechanisms of Transdermal Drug Delivery*, Marcel Dekker, New York, 1997 pp. 1–40.
21. I. H. Patel and R. H. Levy. Absorption kinetics of local anesthetics from rat subcutaneous tissue: II. Effects of vasodilators. *J. Pharmacokin. Biopharm.* **2**:337–346 (1974).
22. P. Singh, R. H. Guy, M. S. Roberts, and H. I. Maibach. What is the transport-limiting barrier in iontophoresis? *Int. J. Pharm.* **101**:R1–R5 (1994).
23. J. Schou. Subcutaneous and intramuscular injection of drugs. In B. B. Brodie and J. R. Gillette (eds), *Handbook of Experimental Pharmacology, Vol. XXVIII, Concepts in Biochemical Pharmacology, Part I*, Springer, Berlin 1971, pp. 47–61.
24. P. Glikfeld, C. Cullander, R. S. Hinz, and R. H. Guy. A new system for *in vitro* studies of iontophoresis. *Pharm. Res.* **7**:443–446 (1988).
25. J. Russo, A. G. Lipman, T. J. Comstock, B. C. Page, and R. L. Stephen. Lidocaine anaesthesia: comparison of iontophoresis, injection, and swabbing. *Am. J. Hosp. Pharm.* **37**:843–847 (1980).
26. P. Glikfeld, R. S. Hinz, and R. H. Guy. Noninvasive sampling of biological fluids by iontophoresis. *Pharm. Res.* **6**:988–990 (1989).
27. P. W. Ledger. Skin biological issues in electrically enhanced transdermal delivery. *Adv. Drug Del. Rev.* **9**:289–307 (1992).
28. T. Hanai and Maku To Ion. 1978, chapter 1, p. 1–37.
29. M. Polásek, B. Gas, T. Hirokawa, and J. Vacik. Determination of limiting ionic mobilities and dissociation constants of some local anaesthetics. *J. Chromatograph.* **596**:265–270 (1992).